INTERNATIONAL JOURNAL OF CLIMATOLOGY
Int. J. Climatol. **34**: 623–642 (2014)
Published online 21 May 2013 in Wiley Online Library
(wileyonlinelibrary.com) DOI: 10.1002/joc.3711

RMetS
Royal Meteorological Society

Updated high-resolution grids of monthly climatic observations – the CRU TS3.10 Dataset

I. Harris,[a] P.D. Jones,[a,b]* T.J. Osborn[a] and D.H. Lister[a]

[a] *Climatic Research Unit, School of Environmental Sciences, University of East Anglia, Norwich, UK*
[b] *Department of Meteorology, Center of Excellence for Climate Change Research, Faculty of Meteorology, Environment and Arid Land Agriculture, King Abdulaziz University, Jeddah, Saudi Arabia*

ABSTRACT: This paper describes the construction of an updated gridded climate dataset (referred to as CRU TS3.10) from monthly observations at meteorological stations across the world's land areas. Station anomalies (from 1961 to 1990 means) were interpolated into 0.5° latitude/longitude grid cells covering the global land surface (excluding Antarctica), and combined with an existing climatology to obtain absolute monthly values. The dataset includes six mostly independent climate variables (mean temperature, diurnal temperature range, precipitation, wet-day frequency, vapour pressure and cloud cover). Maximum and minimum temperatures have been arithmetically derived from these. Secondary variables (frost day frequency and potential evapotranspiration) have been estimated from the six primary variables using well-known formulae. Time series for hemispheric averages and 20 large sub-continental scale regions were calculated (for mean, maximum and minimum temperature and precipitation totals) and compared to a number of similar gridded products. The new dataset compares very favourably, with the major deviations mostly in regions and/or time periods with sparser observational data. CRU TS3.10 includes diagnostics associated with each interpolated value that indicates the number of stations used in the interpolation, allowing determination of the reliability of values in an objective way. This gridded product will be publicly available, including the input station series (http://www.cru.uea.ac.uk/ and http://badc.nerc.ac.uk/data/cru/).

Additional Supporting information may be found in the online version of this article.

KEY WORDS gridded climate data; high resolution; temperature; precipitation

Received 31 July 2012; Revised 1 March 2013; Accepted 30 March 2013

1. Introduction

Mitchell and Jones (2005, hereafter MJ05) updated the earlier high-resolution (0.5° × 0.5° latitude/longitude) monthly datasets initially developed by New *et al.* (1999, 2000). The aim of these three studies was the construction of a globally complete (except the Antarctic) land-only dataset for commonly used surface climate variables. Infilling, to make the dataset as complete as possible, took place based on more distant station data or on relationships with other variables. If no infilling was possible, the value for that variable for the grid box in question relaxed to the 1961–1990 average. That the development was a worthwhile exercise is evident in their citation counts (1380 for MJ05, 1249 for New *et al.*, 1999, and 1318 for New *et al.*, 2000, recorded on Google Scholar in July 2012). The citations, apart from being numerous, are varied covering many fields outside of climate (e.g. agriculture, ecology, hydrology, biodiversity and forestry). MJ05 give some of the history of the datasets. The purpose of this article is twofold: first, to update the datasets to the end of 2009 and to provide the basis for a semi-automated regular updating from 2009 onwards, and second, to include many new station data for earlier periods that have become available over the past 7 years. Some of these station data are homogenized versions that replace station series already existing in the station database. We discuss the datasets that were merged in Section 2 by variable. In Section 3, the interpolation method is introduced, giving details of the procedures in a complex flow diagram. This section includes new 'diagnostics' associated with each gridded value (to indicate the distance from the nearest station or the inter-variable relationship used). Section 4 compares the new version of the dataset with existing gridded datasets, some of which are available at the same resolution, and Section 5 summarizes the main findings.

The processes and procedures described here apply to both versions CRU TS3.00 and CRU TS3.10 of the dataset. CRU TS3.00 was a preliminary version with updates through to summer 2006; it was superceded by CRU TS3.10 when the datasets were updated to

* Correspondence to: P. D. Jones, Climatic Research Unit, School of Environmental Sciences, University of East Anglia, Norwich, NR4 7TJ, UK. E-mail: P.jones@uea.ac.uk

December 2009. All results and statistics shown here were calculated from CRU TS3.10.

2. Data

This updated version (referred to as CRU TS3.10) of MJ05 incorporates the same monthly climatological variables. These are: mean temperature (TMP), diurnal temperature range (DTR) (and so maximum and minimum temperatures, TMX and TMN, calculated as shown in Appendix 3), precipitation total (PRE), vapour pressure (VAP), cloud cover (CLD) and rainday counts (WET). Potential evapotranspiration (PET) is now included in this new version, and is calculated from a variant of the Penman–Monteith formula (http://www.fao.org/docrep/X0490E/x0490e06.htm) using gridded TMP, TMN, TMX, VAP and CLD (see Appendix 1).

2.1. Sources of monthly climate data at the global scale

The principal sources used for the routine updating of the Climatic Research Unit (CRU) monthly climate archives come through the auspices of the World Meteorological Organisation (WMO) in collaboration with the US National Oceanographic and Atmospheric Administration (NOAA, via its National Climatic Data Center, NCDC). We access these products, which appear on a monthly basis in near-real time, through the Met Office Hadley Centre in the UK and NCDC in the USA. Web links to these sources can be found in the supporting information.

- CLIMAT monthly data, internationally exchanged between countries within the WMO. For recent months (the last 2–3 years) there have typically been about 2400 stations but with significant numbers of missing values. We use the term 'missing value' if either the WMO Station Identifier was not present, or a value for a particular variable for that month was set to a missing value code. The actual stations reporting also do not remain constant with time. For example, during the period 2002–2009 (when the average number of stations reporting was around 2200), the overall total number of unique precipitation reporting stations was more than 2800.
- Monthly Climatic Data for the World (MCDW), produced by NCDC for WMO incorporates about 2000 stations. During the period 2002–2009 (when the average number of stations reporting was around 1500), the total number of precipitation reporting stations was about 2600. Thus, as with CLIMAT, the stations that report change with time.
- World Weather Records (WWR) decadal data publications that are exchanged between National Meteorological Services (NMSs) and the archive centre at NCDC. The 1991–2000 version has around 1700 station series. WWR becomes available each decade. These decadal publications, in theory, hold the same data that appears in the monthly publications. In practice, data series (decadal blocks) tend to have fewer missing values and fewer outliers and there are generally more series for some countries. For more specific details about routine updating, see Section 2.2.

The numbers of stations quoted above for CLIMAT and MCDW provide a guide as to the global resources of readily available climate data. WWR data are also publicly available but the provision of the number of stations for each decade is variable as is the case for CLIMAT and MCDW.

2.2. Sources of additional monthly climate data at the national scale

In addition to the systematic incorporation of the above, other opportunities present themselves for new series and/or updates to existing series. Examples here include data exchanges through collaboration with other climate scientists/institutions and releases of climate series (perhaps after homogenization procedures) by National Meteorological Services (NMSs). As examples of the latter, we have been able to replace some of the routine monthly sources with homogeneity-adjusted data series for Australian and Canadian stations. We could add significantly more US stations in real time, but the density from existing CLIMAT and MCDW sources is already greater than for almost all other countries, except for a few small European countries. A major problem with using national sources is that many are supplied without a WMO Station Identifier.

When merging new series from NMS sources, and from WWR and CLIMAT/MCDW, it is necessary to decide the priority one source might have over another, based on data quality considerations. This is also necessary for the near-real-time updating process described in Section 2.4.

The Australian Bureau of Meteorology (BoM) produced 99 non-urban and four urban homogenized temperature series (a link to explanatory material is given in the supporting information). These were merged by matching station series in the TMP archive (with the new values having priority over the old). Additional TMN and TMX station data were also received from BoM for the period 2000–2008. Calculating TMP from TMX and TMN shows small differences when compared with those available from CLIMAT. The differences are due to the CLIMAT data calculating TMP from all observed values in a day as opposed to using $\mathrm{TMP} = (\mathrm{TMX} + \mathrm{TMN})/2$, the method in use up to 1999. Post-1999 TMP CLIMAT data were replaced by using TMP calculated directly from the BoM data (David Jones, BoM, pers. comm. and see also Brohan *et al.*, 2006). Provided a series is calculated consistently, differences between anomalies of TMP calculated from sub-daily observations, and anomalies from TMP calculated from TMN and TMX, will have a zero trend over time. Mixing TMP series when the values have been calculated by different formulae leads to potential inhomogeneities, hence our

efforts to ensure TMP for Australia is calculated in a consistent way throughout time.

The New Zealand NMS supplied 13 homogenized series of mean temperature, which were also merged (new series having priority) (J. Renwick, NIWA, pers. comm.). A link to explanatory material is given in the supporting information.

For Canada, the principal sources are the homogenized series developed by Lucie Vincent (Vincent, 1998; Vincent and Gullet, 1999), together with updates for recent years. Links to sources and further notes are given in the supporting information.

2.3. Homogeneity

The CRU TS dataset is not specifically homogeneous. Whilst many of the observations will have been homogenized (often by national meteorological agencies) prior to publication and use in the process, this is not a requirement for inclusion. With the use of climatological normals (and synthetic data in the case of secondary parameters) to supplement observations, it would be neither appropriate nor straightforward to assess homogeneity throughout the dataset. This dataset should only be used for climate trend analysis, therefore, if the results are treated cautiously, and we recommend that such analysis should be complemented by comparison with other datasets. For example, in Section 4 we compare long-term changes in CRU TS3.10 with CRUTEM3 and GPCC over world regions, and find good agreement at the chosen spatial scales. We also compare CRU TS3.10 mean temperature with CRUTEM4 at that dataset's resolution, finding that long-term ($\sim$50 year) and full-term trends are consistent, with only one or two exceptions where the trends are significantly different at the 95% level.

2.4. Dataset update in near-real time

Figure 1 illustrates the updating procedure using CLIMAT, MCDW and Australian data in near-real time. Each variable is updated in sequence. MCDW is added first, then CLIMAT and finally the Australian BoM data. MCDW and CLIMAT updates usually include many of the same stations. In these cases, the CLIMAT updates take precedence over the MCDW updates.

The procedure is similar for all three data sources. Data are first converted into the CRU database format. They are then merged into the 'Master' database for that variable. The merging process attempts to match 'Update' stations with 'Master' stations, firstly using WMO Station Identifiers, and then metadata (location, elevation, station name, country name) where WMO Station Identifier matching has failed. For CLIMAT data, there are no metadata apart from the WMO Station Identifiers, so this last stage is not possible. Finally a new database is written for each variable, which forms the 'Master' for another stage of updates (see Figure 1).

2.4.1. MCDW publications

MCDW data contains values for monthly mean temperature, vapour pressure, rain days, precipitation and sunshine hours. Cloud cover (as a percentage value) is derived from sunshine hours (see Appendix 3). Where precipitation is given as 'T' (Trace), the value is treated as 0.0. In the CRU TS datasets, the WET variable represents counts of wet days defined as having $\geq$0.1 mm of precipitation. Therefore, wet day counts are converted from RDY (days with $\geq$1 mm of precipitation) to RD0 (usually days with $\geq$0.1 mm of precipitation) using relationships derived by New *et al.* (1999) and described in the supporting information. Some other climatological variables are included in MCDW (e.g. surface and station level pressure) but not used here. Metadata consists of WMO Station Identifier, station name, latitude, longitude and elevation. The resulting 'MCDW databases' for TMP, PRE, VAP, WET and CLD (derived from sun hours) are then merged into the relevant current databases for the next stage.

2.4.2. CLIMAT messages

CLIMAT messages contain values for monthly mean temperature, vapour pressure, rain days, precipitation, sunshine hours and minimum/maximum temperatures. Again, cloud cover (as a percentage value) is derived from sunshine hours (see Appendix 3), provided a valid latitude for the conversion can be found: metadata is restricted to a WMO Station Identifier, necessitating matching against a reference list of WMO stations to obtain latitude, longitude and other information. Wet days are converted from RDY to RD0 (see Section 2.4.1.). As with MCDW, there are a number of additional fields that are not used.

The resulting 'CLIMAT databases' for TMP, PRE, VAP, WET and CLD (from sun hours) are then merged into the interim databases from the previous MCDW merge operations, forming the new databases for those variables. The CLIMAT databases for TMN and TMX are merged into the appropriate current databases, forming new versions for the final ('BoM') stage.

2.4.3. BoM data

The Australian Bureau of Meteorology (BoM) data contain only values for minimum and maximum temperature (in separate monthly files). Metadata are restricted to a local identifier (not a WMO Station Identifier), with latitude, longitude and elevation. Thus each entry must be matched with an existing, WMO-coded CRU TS station. This is assisted by augmenting the database header lines of those stations with the BoM local identifier. This positively links that database station with one of the BoM-coded stations. The minimum and maximum temperature values are processed in parallel and as stated earlier TMP is calculated from TMN and TMX by simple averaging. The resulting BoM databases for TMN and TMX are then merged with the appropriate databases from the previous stage, forming the latest TMN and TMX databases. The BoM data files, as received, are not available online.

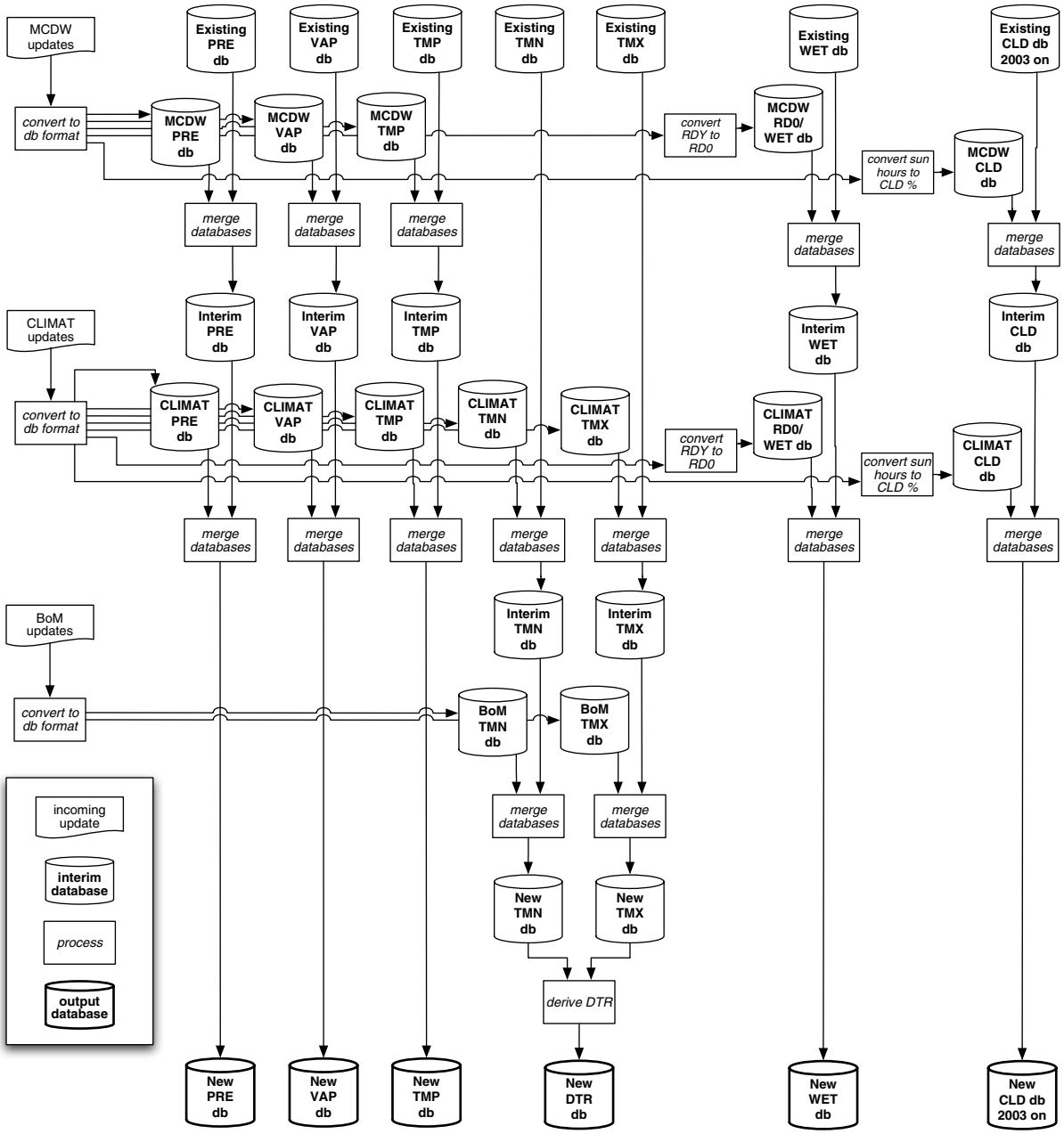

Figure 1. Database update flowchart. This shows how updates from MCDW, CLIMAT and BoM are incorporated into the existing databases of weather station records.

2.4.4. Derivation of DTR

The new current TMN and TMX databases are arithmetically processed to produce the new current DTR database.

3. Gridding the station data to the regular latitude/longitude grid

CRU TS uses a global grid, with resolution 0.5° longitude by 0.5° latitude, and data is provided for land cells only. The Terrainbase 5′ elevation database (described in the supporting information) is used to determine land cells: only if all 36 Terrainbase gridcells are marked as 'ocean', will the enclosing CRU TS grid cell be marked as 'ocean'. Antarctica is, exceptionally, also marked as ocean. This process is described by New *et al.* (1999). The next section describes the gridding procedure in a series of steps. The whole process is depicted as a flowchart in Figure 2.

3.1. Usable and anomaly data

The CRU TS datasets are constructed using the Climate Anomaly Method (CAM, Peterson *et al.*, 1998a). To be included in the gridding operations, therefore, each station series must include enough data for a base period average, or normal, to be calculated. The base period is 1961–1990 (unless otherwise stated), and a minimum of 23 non-missing values (i.e. over 75%) over this period, in each month, is required for a normal to be calculated

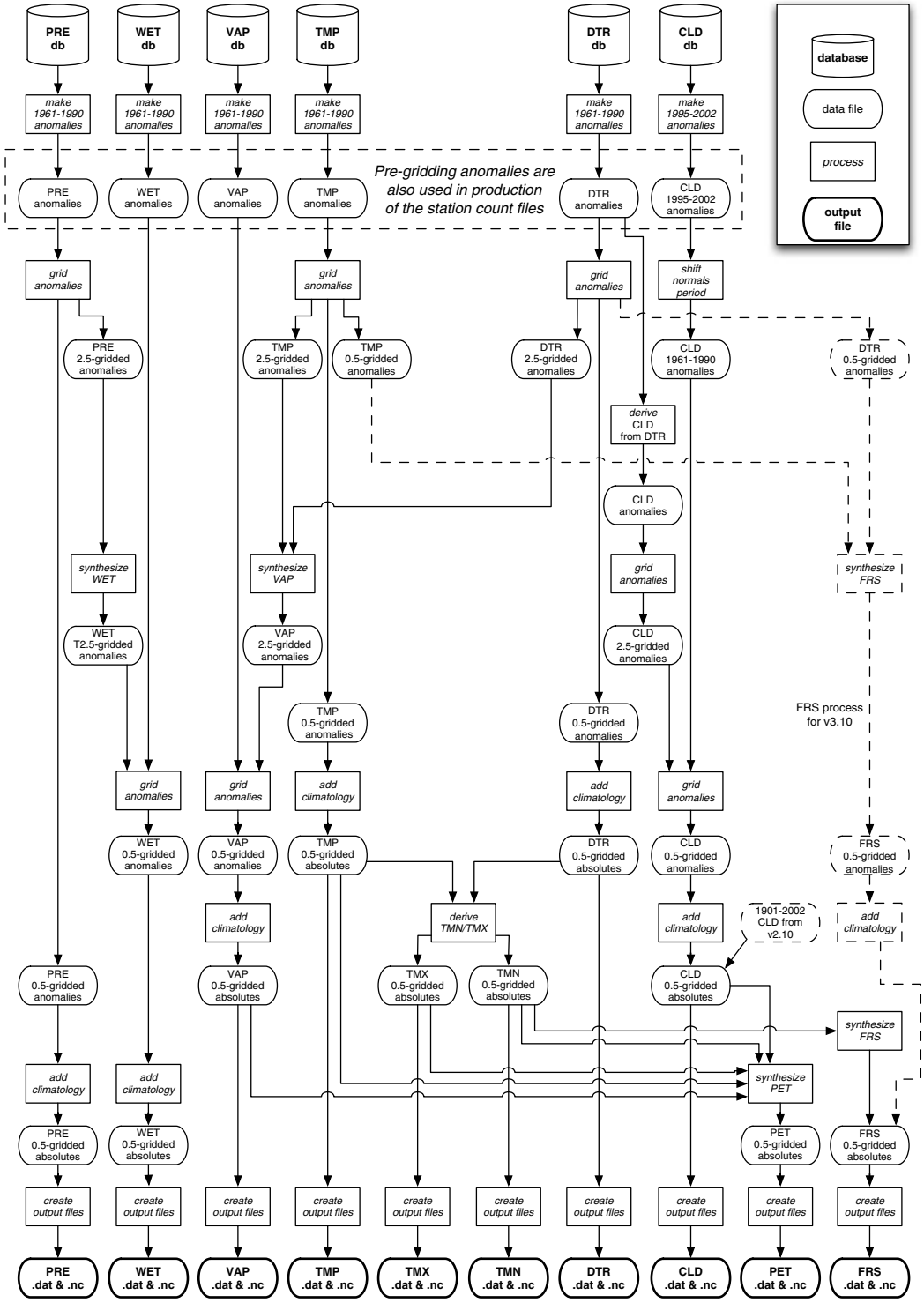

Figure 2. Gridding Process. Demonstrating the sequence of processes that derive the final gridded data products from the station databases. The FRS process for CRU TS 3.10 is illustrated by dashed lines (Section 3.3.6.).

for that month. Where normals can be produced for any month, values for that month in the station series are used in the gridding process, provided they are not identified as outliers. Outliers are defined as values that fall more than 3.0 standard deviations from the normal, (4.0 for precipitation). Thus, standard deviations are also calculated for each month for each station series to enable outlier screening. The result of these exclusions in each region is shown in Figure 3. For some continents, almost one half of the station data are not used because the base periods are not sufficiently complete to estimate normals. Only a very small percentage (<1%) of values are excluded as outliers.

Each station series passed for inclusion into the gridding process is converted to anomalies by subtracting the 1961–1990 normal from all that station's data, on a

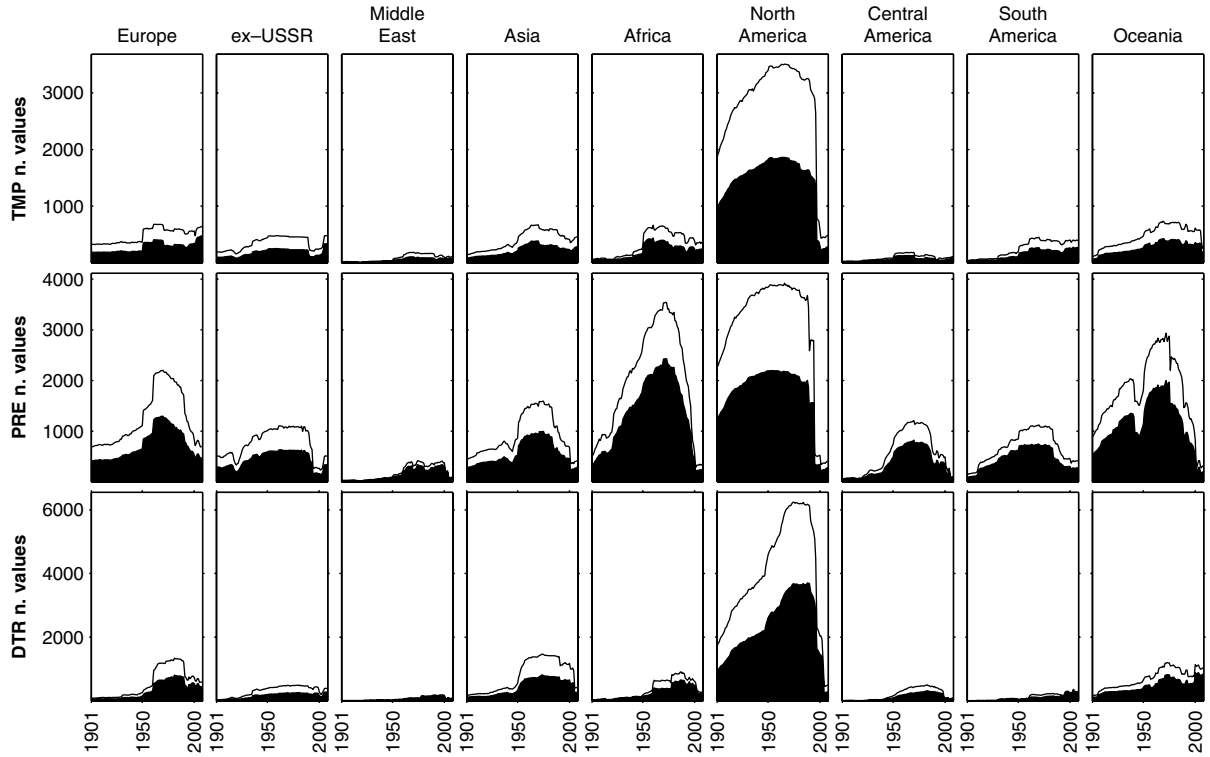

Figure 3. The number of data values per month, for the three primary variables (TMP, PRE and DTR) actually used (shaded) and the total in the databases (top line). The monthly numbers are smoothed with a Gaussian-weighted filter (width = 13). These values may be used as a proxy for station numbers, since the incidence of potentially duplicate stations (based on spatial metadata) is low (about 1% for TMP, 2.3% for DTR and 0.6% for PRE).

monthly basis (see Willmott and Robeson, 1995, who refer to this as Climatically-Aided Interpolation). In anomaly form, station climate data are in much better agreement with little dependence on elevation evident. The exceptions to this simple subtraction rule are:

- precipitation and rain days, for which percentage anomalies are calculated. These express percentage change from the normal, such that a value equivalent to the normal gives rise to an anomaly of 0%. A value of zero gives rise to an anomaly of −100%, the lowest possible anomaly for variables such as PRE and WET. The percentage anomaly equations are shown in Appendix 2.
- cloud cover, for which anomalies are initially calculated relative to a 1995–2002 mean, and then converted to 1961–1990 anomalies (owing to sparseness of data). See Section 3.3.4. for more information.

3.2. Coverage

The influence of station data in each half-degree land grid cell varies with time and between variables. Table II of MJ05 defines correlation decay distances (CDDs) for each variable, which are used to indicate the potential information that might be obtained from each station location. The calculation of these values is documented by New *et al.* (2000). The CDDs range from 1200 km for TMP to 450 km for PRE. Two diagnostics are provided (see Section 3.4.) for every variable, grid cell and time step. First, 'station counts' (SC) indicate the number of station values that lie within each grid cell. Second, 'station influences' (SI) indicate the number of station values that are within the CDD from the centre of each grid cell. Any half-degree land cell is defined as having station data if it falls within the CDD of at least one station with a value for that time step (i.e. $SI \geq 1$). Figure 4 shows the percentage of cells with $SI \geq 1$ in each region, also identifying cells that actually contain a station ($SC \geq 1$). The remainder (above the black filled areas in Figure 4) are land grid cells with no observations within the CDD of their centre. The vast majority of half-degree cells are filled with data interpolated from stations that are outside the cell but lie within the CDD range for the particular variable. Less interpolation occurs for PRE and also DTR, as CDDs for these variables are shorter.

3.3. Gridding anomalies

Given that the primary purpose of the dataset is to provide full coverage of the specified continental land areas, with no missing data, the gridding process is complex. A flowchart of the procedure is given in Figure 2.

At each time step, the input data are the available station anomaly values and the station locations. The CDD for the variable in question is then used with these locations to identify any global cells (at $2.5^\circ \times 2.5^\circ$ resolution) which are not influenced by any station. This coarser grid size is used for efficiency purposes, since this cell size is still less than any variable CDD, so

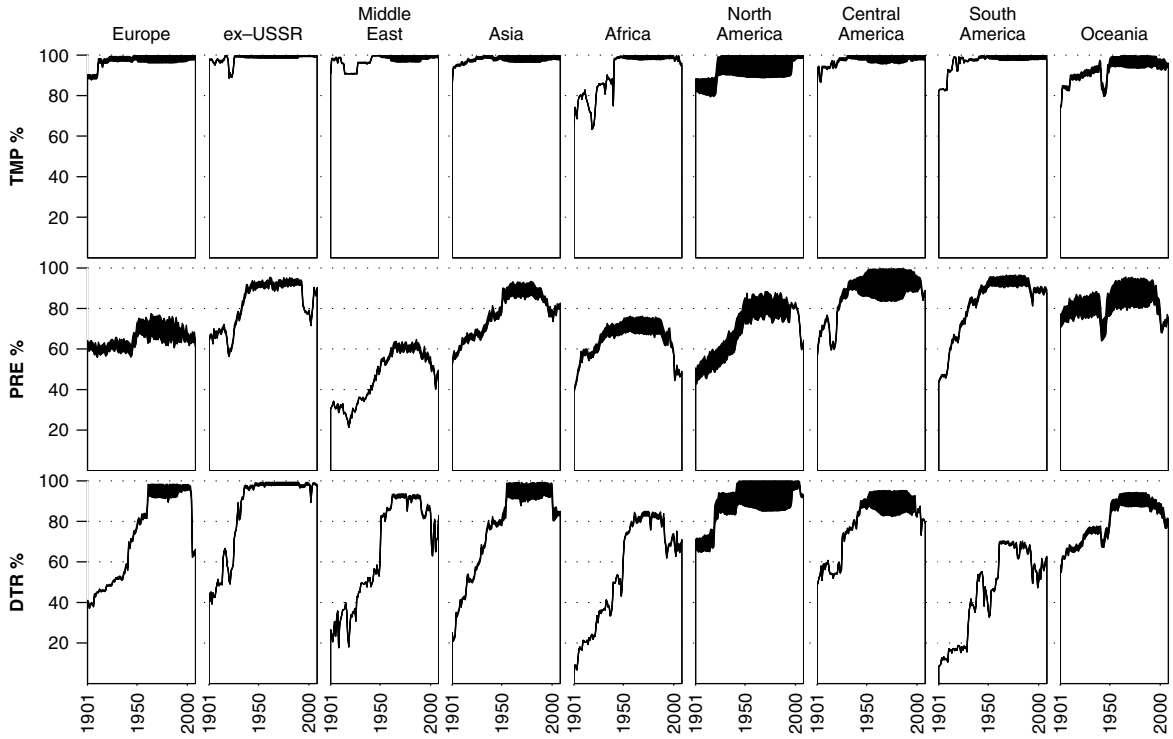

Figure 4. The percentage of half-degree land cells, for the three primary variables (TMP, PRE and DTR) containing stations with valid values (black) or within the CDD of those stations (white). Data are monthly, smoothed with a Gaussian-weighted filter (width = 13).

total coverage can be fulfilled at this resolution. What happens to these grid cells depends on the variable. For primary variables (PRE, TMP, DTR), the 'empty' cells are populated with dummy stations, which are given a zero anomaly value. Since anomalies are being processed, this is equivalent to inserting the climatology value for that cell and month (because the climatology is added at the end of the process, to give absolute values in the datasets). For secondary variables, there is typically less station coverage than for primary variables, so any available synthetic data (derived from primary variables and described in Appendix 3) are used to populate empty cells. This approach is described for VAP, WET and FRS by New *et al.* (2000), referenced in MJ05, and is used here to preserve consistency with earlier versions of the dataset. Additionally, it lessens the chance of users calculating these variables themselves in differing ways. Any cells remaining empty after this operation are populated by dummy stations with zero anomalies (as for primary variables). The gridding is performed globally, so dummy stations are always required over oceans and Antarctica. Only land cells north of 60°S are retained.

The gridding operation itself is triangulated linear interpolation, producing values on a grid with half-degree resolution. This is undertaken using the IDL™ routines 'triangulate' and 'trigrid' (IDL is a trademark of ITT Corporation; supporting information contains a link). 'Triangulate' constructs a Delaunay triangulation of the station locations, returning a list of the coordinates of the vertices of each triangle. A Delaunay triangulation is not well defined when many points lie on a straight line, which is the case where large numbers of dummy stations are provided on a regular 2.5° by 2.5° grid over the oceans, Antarctica and regions more than the CDD from any station observations. In these cases, small deviations are added to the locations of the dummy stations. The results of 'triangulate' are passed to 'trigrid', along with the anomaly data, the desired grid spacing, and the spatial limits. The spatial limits are given as half a grid cell within 180°W to 180°E by 90°S to 90°N. 'Trigrid' returns a regular grid of interpolated values using linear interpolation within each triangle. Other, more sophisticated gridding algorithms are available (see, e.g. Hofstra *et al.*, 2008, who investigated six methods of interpolation across Europe, finding little difference in results using a number of measures of their interpolation skill). Our approach was chosen to be consistent with the previous version of the dataset. The monthly station observations for TMP, TMN, TMX and PRE, on which this dataset is based, will be made available alongside the dataset itself through BADC (Section 5).

The next subsections describe the gridding process, and subsequent conversion to absolute values and formatted output files. These processes differ for certain variables. In all cases, the term 'climatology' is used to refer to the gridded 1961–1990 normals (New *et al.*, 1999) used with all earlier versions of the CRU TS dataset. These are distinct from the normals calculated earlier on a per-station basis, which allowed station anomalies to be calculated.

3.3.1. Precipitation (PRE), temperature (TMP) and diurnal temperature range (DTR)

Monthly station anomalies are passed to the gridding routine, which produces half-degree gridded anomalies. These are then converted to absolute values. For TMP and DTR, this involves the addition of the monthly gridded climatology. For PRE, the gridded percentage anomalies are multiplied by the climatology, divided by 100, and then the climatology is added (Appendix 2). For PRE and DTR, any negative values are set to zero. Finally the absolute values are formatted for output.

3.3.2. Vapour pressure (VAP)

Monthly TMP and DTR station anomalies are also gridded (using the same triangulation method) to a coarser $2.5^\circ \times 2.5^\circ$ grid. From these, anomalies of vapour pressure are estimated using a semi-empirical formula and an assumption that the dew-point temperature anomalies are equivalent to the minimum temperature anomalies (see Appendix 3). We call these values, estimated from the TMP and DTR gridded anomalies, 'synthetic' VAP anomalies. These are passed, together with observed VAP anomalies from the VAP station database, to the gridding routine to produce half-degree gridded anomalies. The half-degree gridded VAP anomalies are, therefore, produced by interpolation (Section 3.3.) from the observed station VAP with support from the coarsely gridded synthetic VAP in regions where there are observations of TMP and DTR but not VAP. These are then converted to absolute values by the addition of the monthly gridded climatology, and any negative values are set to zero. Finally, the gridded absolutes are formatted for output.

3.3.3. Rain days (WET)

Monthly PRE station anomalies are also gridded (using the same triangulation method) to a coarser 2.5° by 2.5° grid. From these, anomalies of WET are estimated using the empirical formula derived by New *et al.* (2000) shown in Appendix 3, to produce 'synthetic' WET anomalies at the same resolution. The synthetic WET anomalies are then passed, together with observed WET anomalies from the WET station database, to the gridding routine to produce half-degree gridded anomalies. The gridded WET percentage anomalies are then converted to absolute values with the same process used for PRE (Section 3.3.1.), and then restricted to ensure that they lie between zero and the number of days in the month in question. The gridded absolutes are finally formatted for output.

3.3.4. Cloud cover (CLD)

For years up to and including 2002, the CLD published product is static (i.e. the values from CRU TS2.10 are used). For 2003 onwards, DTR station anomalies are used to estimate 'synthetic' CLD station anomalies, by a linear transformation with a scaling factor and mean offset calculated from CRU TS2.10 gridded CLD and DTR values for each latitude band (see Appendix 3). These are passed to the gridding routine, producing 2.5-degree gridded synthetic CLD anomalies. Separately, observed CLD anomalies from the CLD station database are produced based on the normal period 1995–2002. These anomalies are then adjusted to represent anomalies based on 1961–1990, by subtracting the difference between the means of the two periods calculated from the CRU TS2.10 published data, for each grid cell and month. The two sets of CLD anomalies are then passed to the gridding routine, which uses the synthetic CLD to support the observed CLD, and produces half-degree gridded anomalies. These are then converted to absolute values by the addition of the monthly gridded climatology, and restricted to lie between 0 and 100 %. The absolute values are then formatted for output. Deriving CLD from DTR maximizes consistency with earlier versions of the dataset. Although sunshine duration observations are now available in sufficient numbers to allow Sun Hours to be introduced as a variable, this is not the case for older data.

3.3.5. Minimum and maximum temperature (TMN, TMX)

TMN and TMX are derived arithmetically from gridded absolute values of TMP and DTR (see Appendix 3), and formatted for output. This approach results in TMN and TMX values having a fixed and predictable relationship with TMP and DTR. The observed values of TMN and TMX are represented by DTR and TMP. TMN and TMX are not referred to as either primary nor secondary variables, as they are simple calculations from TMP and DTR.

3.3.6. Frost days (FRS)

For CRU TS3.10, gridded anomalies of the number of frost days (FRS) are estimated entirely synthetically from an empirical function of TMP and DTR half-degree gridded anomalies (see Appendix 3). These are then converted to absolute values by the addition of the monthly gridded climatology, and limited to realistic day counts for each month (as for WET, Section 3.3.3.). The gridded absolute values are finally formatted for output. This process has been substantially improved by deriving FRS synthetically from gridded absolute TMN, thus ensuring a realistic relationship between FRS and TMN. This will form part of the next CRU TS version.

3.3.7. Potential Evapotranspiration (PET)

Potential Evapotranspiration (PET) is derived from half-degree gridded absolute values of TMP, TMN, TMX, VAP and CLD, and from a fixed monthly climatology for wind speed (New *et al.*, 1999) (a brief investigation of the effect of using a fixed climatology for wind speed may be found in the supporting information). These gridded values are calculated using a variant of the Penman-Monteith method (see Appendix 1) to estimate

PET at the same resolution. These gridded absolute values of PET are then formatted for output. Note that because of the reduced land coverage of the wind speed climatology, PET is not available for all CRU TS land cells. The 'missing' areas are principally small islands and coastlines, where the fixed monthly climatology for wind speed is not available (New *et al.*, 1999).

3.4. Station counts

In order to allow users of the dataset to assess the robustness of a particular datum (i.e., the value in one grid cell in one month and year), station count files are provided. They are the same size and format as the data files, and there are two types of station count (Section 3.2.). The first (station influences, SI) is suffixed 'stn', and indicates the number of stations that could have influenced the datum, that is, how many stations within the CDD were reporting a valid value at that time step. Only stations at the vertices of the triangle that encompass the centre of the grid cell actually contribute, and if SI < 3 then the stations are augmented by dummy stations with zero anomalies (see Section 3.3.), which act to diminish the amplitude of the grid cell anomaly. The second (station counts, SC) is suffixed 'st0', and is the number of stations located within the cell in question reporting a valid value at that timestep. For CLD, as for the variable values, the station influences from 1901–2002 are static and replicated from the 2.10 release. As this did not include 'st0', station counts are not available for CLD until 2003. Station counts are produced for TMP, DTR, PRE, VAP, WET and CLD. Additionally, combined counts are produced for TMP/DTR, to give an indication of their combined contributions. This allows overall station contributions to be assessed for VAP (which uses synthetic VAP constructed from TMP and DTR), and TMN, TMX and FRS (which are derived entirely from TMP and DTR). Station contributions for WET can be assessed by examining the counts for PRE and WET. The station counts process is shown in Figure 5.

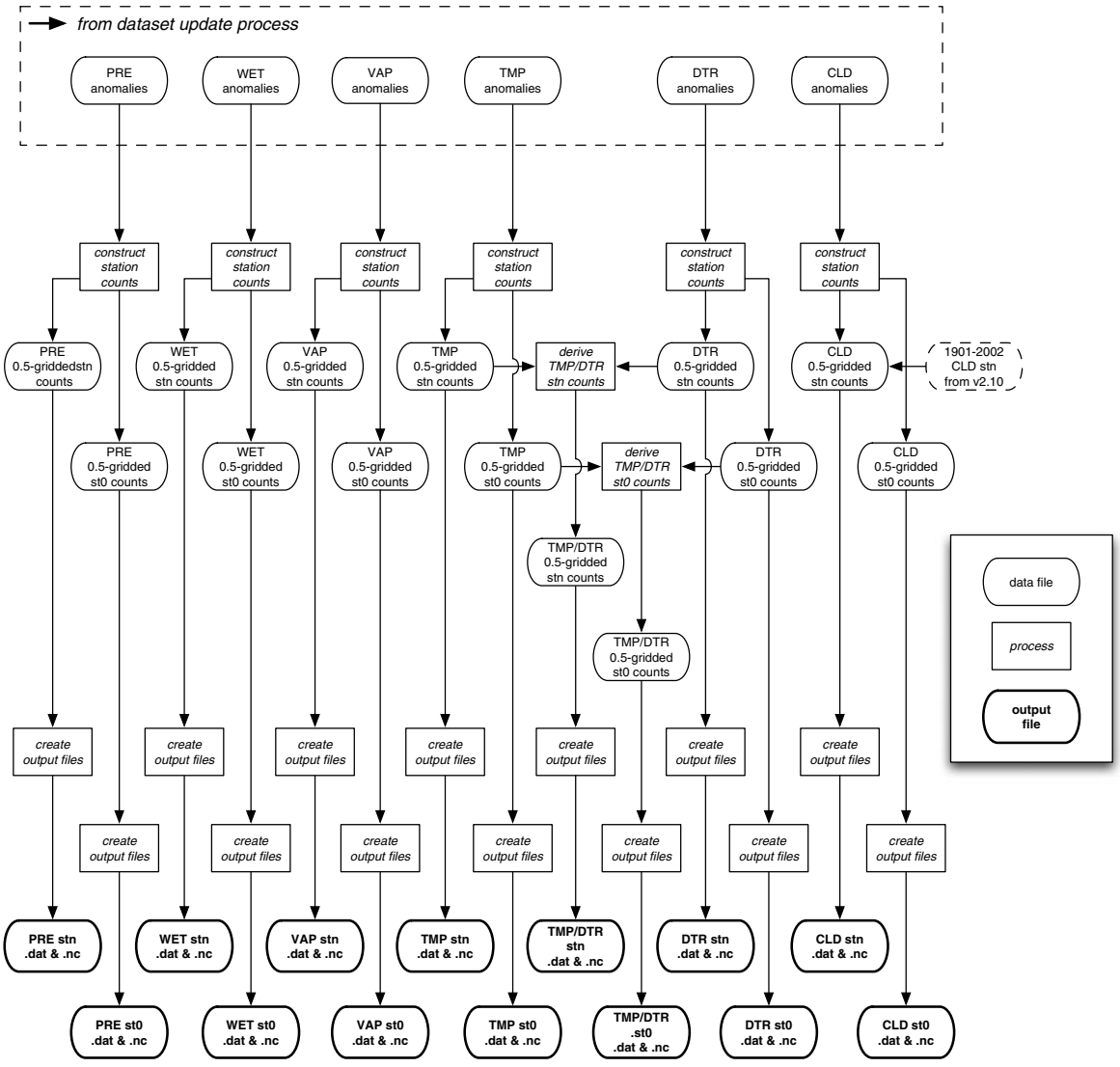

Figure 5. Station Counts Gridding Process. Showing the process by which the station count files are produced as part of the main dataset update process.

4. Comparisons with other datasets

4.1. Sub-continental scales

In this section we compare our new CRU TS3.10 dataset with two similarly highly-spatially-resolved datasets for mean temperature and precipitation. For temperature, we use version 2.01 (1900–2008) of the dataset developed by the University of Delaware (UDEL), which is based on the GHCN-M (Peterson and Vose, 1997; Peterson *et al.*, 1998b) and GSOD datasets. UDEL is used because it is at the same spatial resolution as CRU TS. For precipitation, we compare with version 5 (1901–2009) of the precipitation dataset developed by Global Precipitation Climatology Centre (GPCC: Becker *et al.* 2013; Schneider *et al.* 2013). UDEL also has a precipitation dataset, but the GPCC product uses considerably more stations than either UDEL or CRU TS3.10. Both datasets are described, and can be downloaded from, websites listed in the supporting information.

We do not know which stations are used for either UDEL or GPCC, though the main sources are given. GPCC releases a number of data products, but they do not release the original station data due to agreements DWD have entered into with the other NMSs that provided the data. GPCC is a German contribution to the World Climate Research Programme (WCRP) and to the Global Climate Observation System (GCOS).

Table 1 gives long-term trends of the annual-mean temperature series for the selected regional averages over the full period of record (1901–2008) and the temporal correlations between the two datasets for each of the 20 regions. The selected regions are taken from those introduced by Giorgi and Francesco (2000). Table 2 shows the precipitation trends for the same regions over two periods (1951–2009 and 1901–2009), again with correlations between the annual-mean precipitation from the two datasets.

Figure 6 shows graphical comparisons for regional mean temperature and Figure 7 for precipitation. The same temperature and precipitation scales (°C anomaly from 1961–1990 for temperature, and % anomaly from 1961–90 for precipitation) are used for all of the regions, except for precipitation in the Australian regions, which have a different scale owing to their comparatively-high variability. Differences in year-to-year variability relate to the size of the region and inherent interannual variability of that region. For temperature, more poleward regions are more variable, while for precipitation, the greatest variability is evident across the smaller Australian regions.

Table 1. Region definitions, long-term temperature trends (°C/decade) and correlations between annual-mean temperature timeseries from CRU TS3.10 ('CRU') and UDEL or CRUTEM3. Trends significant at the 95% level are given in bold. Trend and significance values are obtained using iteratively reweighted least squares with a bisquare weighting function, 'robustfit', in Matlab (v.7.9.0, The MathWorks Inc., Natick, MA, 2009).

Region	Lat/Lon Limits				Temperature		Corr
	S	N	W	E	Trend °C/decade 1901–2008		
					CRU	UDEL	
Alaska	60	72	−170	−103	**0.13**	**0.13**	0.98
Central North America	30	50	−103	−85	**0.05**	0.02	0.98
Eastern North America	25	50	−85	−50	**0.07**	0.03	0.96
Western North America	30	60	−135	−103	**0.11**	**0.08**	0.98
Central America	10	30	−116	−83	**0.09**	**0.06**	0.88
Amazon	−20	12	−82	−34	**0.04**	**0.06**	0.87
Southern South America	−56	−20	−76	−40	**0.05**	**0.05**	0.96
Northern Europe	48	75	−10	40	**0.10**	**0.07**	0.99
Mediterranean Basin	30	48	−10	40	**0.10**	**0.05**	0.92
Western Africa	−12	22	−20	18	**0.05**	**0.04**	0.80
Eastern Africa	−12	18	22	52	**0.05**	**0.05**	0.88
Southern Africa	−35	−12	10	52	**0.05**	**0.06**	0.91
North Asia	50	70	40	180	**0.13**	**0.09**	0.98
Central Asia	30	50	40	75	**0.13**	**0.09**	0.98
Southern Asia	5	50	64	100	**0.09**	**0.07**	0.96
East Asia	20	50	100	145	**0.11**	**0.06**	0.94
Southeast Asia	−11	20	95	115	**0.03**	0.01	0.73
Northern Australia	−30	−11	110	155	**0.06**	**0.05**	0.97
Southern Australia	−45	−30	110	155	**0.09**	0.02	0.84
Australia	−45	−11	110	155	**0.06**	**0.04**	0.95
					CRU	CRUTEM3	
Northern Hemisphere	0	90	180	180	**0.10**	**0.09**	0.97
Southern Hemisphere	−60	0	180	180	**0.05**	**0.08**	0.94
Global	−60	90	180	180	**0.07**	**0.08**	0.97

Table 2. Long-term regional precipitation trends (mm/decade) and correlations between annual-mean regional precipitation timeseries from CRU TS3.10 ('CRU') and GPCC. Trends significant at the 95% level are given in bold. Regions are defined and trends are calculated as for Table 1.

Region	Precipitation trend (mm/decade)								
	1901–1950		Corr	1951–2009		Corr	1901–2009		Corr
	CRU	GPCC		CRU	GPCC		CRU	GPCC	
Alaska	1.10	1.68	0.74	0.27	0.65	0.88	−0.03	0.37	0.79
Central N. America	0.86	0.89	1.00	**2.13**	**1.94**	0.99	**0.92**	**0.80**	0.99
Eastern N. America	0.31	0.69	0.97	**1.33**	**0.96**	0.97	**0.93**	**0.85**	0.97
Western N. America	−1.01	−0.46	0.91	0.19	0.36	0.95	0.35	**0.45**	0.93
Central America	0.85	−0.15	0.70	0.85	−0.11	0.83	**0.68**	−0.17	0.72
Amazon	−0.18	**1.22**	0.74	**0.94**	0.34	0.85	0.24	0.26	0.78
Southern S. America	1.09	0.05	0.93	**1.46**	**1.20**	0.97	**1.15**	**0.72**	0.94
Northern Europe	0.52	0.14	0.99	**1.60**	**1.68**	0.99	**0.91**	**0.86**	0.99
Mediterranean Basin	−1.33	**−1.97**	0.94	−0.76	−0.87	0.97	−0.33	**−0.48**	0.96
Western Africa	0.19	**−1.43**	0.82	**−2.15**	**−2.99**	0.94	**−0.70**	**−1.42**	0.89
Eastern Africa	0.21	0.64	0.92	−0.60	**−0.97**	0.87	−0.04	−0.24	0.89
Southern Africa	0.29	0.49	0.90	**−0.86**	**−1.38**	0.90	0.01	−0.25	0.89
North Asia	**1.57**	**1.98**	0.91	0.29	**0.81**	0.89	**0.92**	**1.66**	0.91
Central Asia	−0.26	**−1.56**	0.89	0.09	−0.04	0.94	**0.62**	0.29	0.92
Southern Asia	**1.35**	**−1.33**	0.26	−0.11	0.05	0.91	0.12	**−0.91**	0.53
East Asia	0.35	−0.01	0.94	−0.68	**−1.12**	0.93	0.05	−0.19	0.93
Southeast Asia	0.48	−0.33	0.83	−0.10	−0.19	0.89	0.02	−0.27	0.86
North Australia	−0.73	−0.67	0.99	2.16	2.25	0.99	0.87	0.57	0.99
South Australia	0.98	0.56	1.00	−2.15	−1.61	0.99	0.39	0.15	0.99
Australia	−0.52	−0.61	0.99	1.18	1.50	0.99	0.77	0.47	0.99
Northern Hemisphere	**0.49**	0.10	0.81	0.16	0.07	0.88	**0.24**	**0.30**	0.86
Southern Hemisphere	−0.31	**1.09**	0.78	0.40	0.09	0.90	**0.28**	0.16	0.84
Global	**0.34**	**0.47**	0.78	0.25	0.06	0.88	**0.26**	**0.28**	0.87

In Figure 6, the agreement between the two temperature datasets is excellent for all 20 regions. This result is expected, as the datasets use similar sources of data. UDEL is based principally on Global Historical Climatology Network – Monthly (GHCN-M) and the related Global Summary of the Day (GSOD) dataset (Cort Willmott, pers. comm., 20 May 2009). Correlations between the two datatsets (Table 1) are in the range 0.73 to 0.99, with only two regions below 0.84 (0.73 for southeast Asia and 0.81 for western Africa). Our knowledge of temperature variability on spatial scales of this size (see discussion in Jones *et al.*, 1997, 2001), particularly the number of spatial degrees of freedom, clearly indicates that once the number of stations (assuming they are well-spaced spatially) is 'sufficient', extra numbers barely affect regional averages. More station numbers will, however, help with spatial detail at smaller scales (particularly at the grid-box scale). For regions with high station numbers, such as Europe and North America, it is difficult to tell the two lines apart, and correlations exceed 0.94 for eleven regions. Greater differences occur for lower latitude regions (e.g. Central America, Amazon, the African regions and Southern Asia).

The agreement between the new CRU TS3.10 regional precipitation and GPCC v5 data (Figure 7) is again excellent, though not quite as good as for the temperature comparisons (mean correlation of all regions excluding NH, SH and global is 0.92 for temperature and 0.89 for precipitation). Differences are greatest for the following regions: Alaska, Central America, all African regions since the late 1990s, and Northern and Southern Asia for the first half of the twentieth century. Despite these differences, the agreement is notable because CRU TS3.10 uses a much smaller number of station records than GPCC. Since 1901, the number of stations in CRU TS3.10 is less than half that in GPCC and only about 30% of the GPCC total since about 1980. Maps of GPCC station data coverage indicate that it is very dense in some countries of the world, but in others it is comparable to CRU TS3.10.

Correlations (Table 2) between the 20 pairs of regions are in the range 0.53 to 0.99 with only four series below 0.84 (0.79 for Alaska, 0.72 for Central America, 0.78 for the Amazon and 0.53 for southern Asia). The regions with lower correlations show greatest differences in the earliest years, especially before the 1930s, or in the last 10 to 20 years. Restricting the comparison to 1951–2009 raises these correlations to 0.83 or higher. Indeed, 18 out of the 20 regional correlations are as high or higher over 1951–2009 than over the longer 1901–2009 period. The highest correlations between CRU TS3.10 and GPCC v5 precipitation are evident for regions with the greater stations counts in CRU TS3.10 (compare Figure 7 with Figure 3).

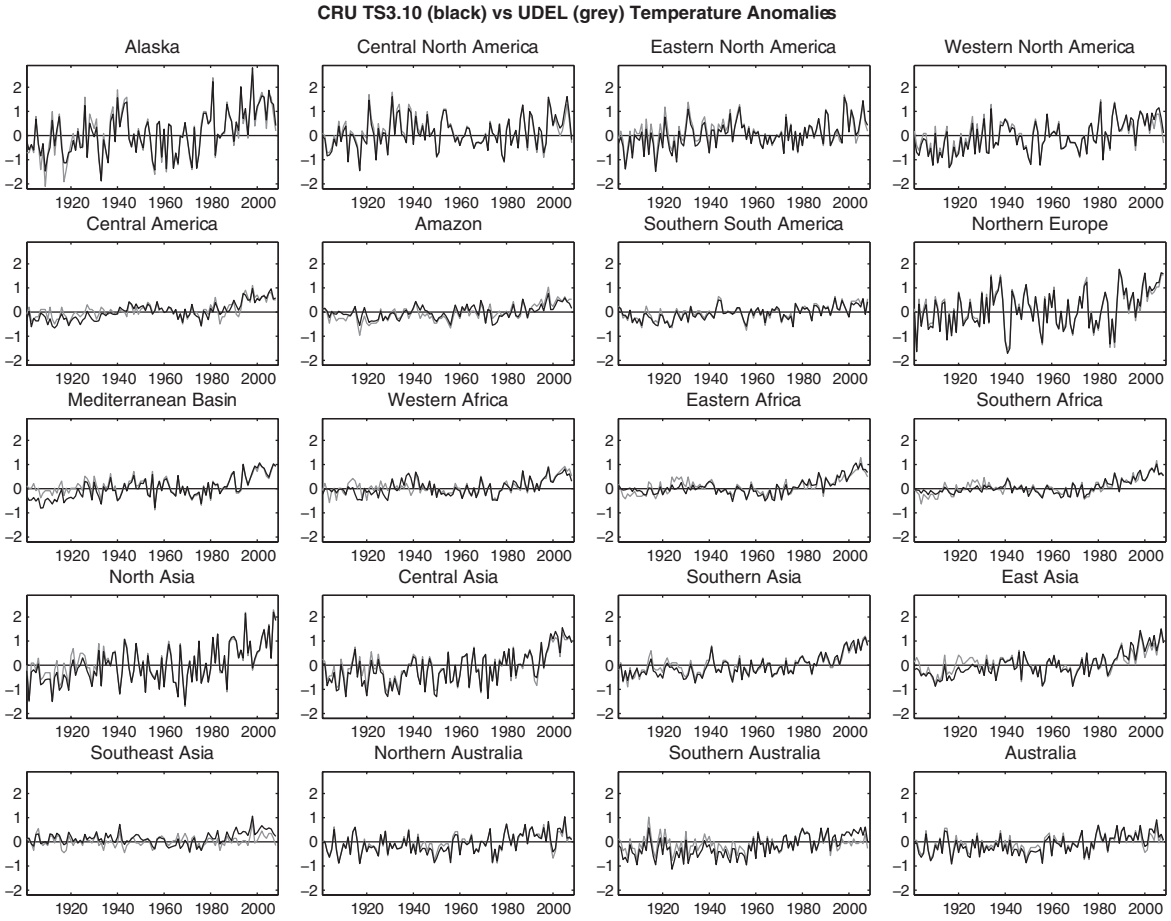

Figure 6. Regional comparisons between CRU TS3.10 (black lines) and UDEL (grey lines) for mean annual temperature anomalies (°C), 1901–2008. Values are plotted as anomalies from the 1961–90 base period, using the same scale for all regions.

4.2. Australia

We have paid particular attention to getting additional data for Australia. In this section, we compare temperature (TMP, TMN and TMX) with national averages for Australia developed by BoM (Figure 8). Australian national averages are considered reliable only since 1910 as there are known issues with exposure changes before 1910 for some Australian states (see the discussion in Nicholls *et al.*, 1996). The series correlate highly, but the overall trends are stronger for BOM than for CRU TS3.10, especially for maximum temperature (Table 3). The differences in recent years (Figure 8) appear to relate to the reporting of TMP over the CLIMAT system by BoM (see earlier discussion in Section 2.2).

4.3. Hemispheric and global scales

4.3.1. Mean temperature

We compare CRU TS3.10 mean temperatures with the coarser resolution datasets CRUTEM3, developed in Brohan *et al.*, 2006, and CRUTEM4 (Jones *et al.*, 2012). Links to these datasets are given in the supporting information. CRUTEM3 was utilized for hemispheric comparisons; CRUTEM4 for a more spatially detailed analysis of trends, in the final paragraph of this section.

For the NH and SH, we have calculated annual land-based averages from CRU TS3.10. For the SH, the CRUTEM3 series includes the Antarctic after the mid-1950s, while this is absent from CRU TS3.10. Figure 9 shows the comparisons, and Table 1 gives the correlations between the series and the trends over the period 1901–2008. When looking at Figure 9 it is vital to remember that the hemispheric series produced in this paper are for all land areas (north of 60°S), whereas the CRUTEM3 series only uses grid boxes (at $5^\circ \times 5^\circ$ resolution) where there are data values. The impacts of this affect the hemispheres differently.

For the NH, the CRU TS3.10 series developed here is warmer than CRUTEM3, particularly so for the warmest years. This is likely due to the infilling of land areas, particularly in higher latitudes over North America and northern Asia, from surrounding stations within the specified CDDs. These regions show quite strong positive anomalies in recent years, and the interpolation to infill values across all grid cells yields a warmer average temperature for CRU TS3.10 compared with CRUTEM3, which does not interpolate to infill the (coarser resolution) grid cells that do not contain any station data (see also Jones *et al.*, 2012). Despite this, the 1901–2009 trends are similar (Table 1), however, because CRU

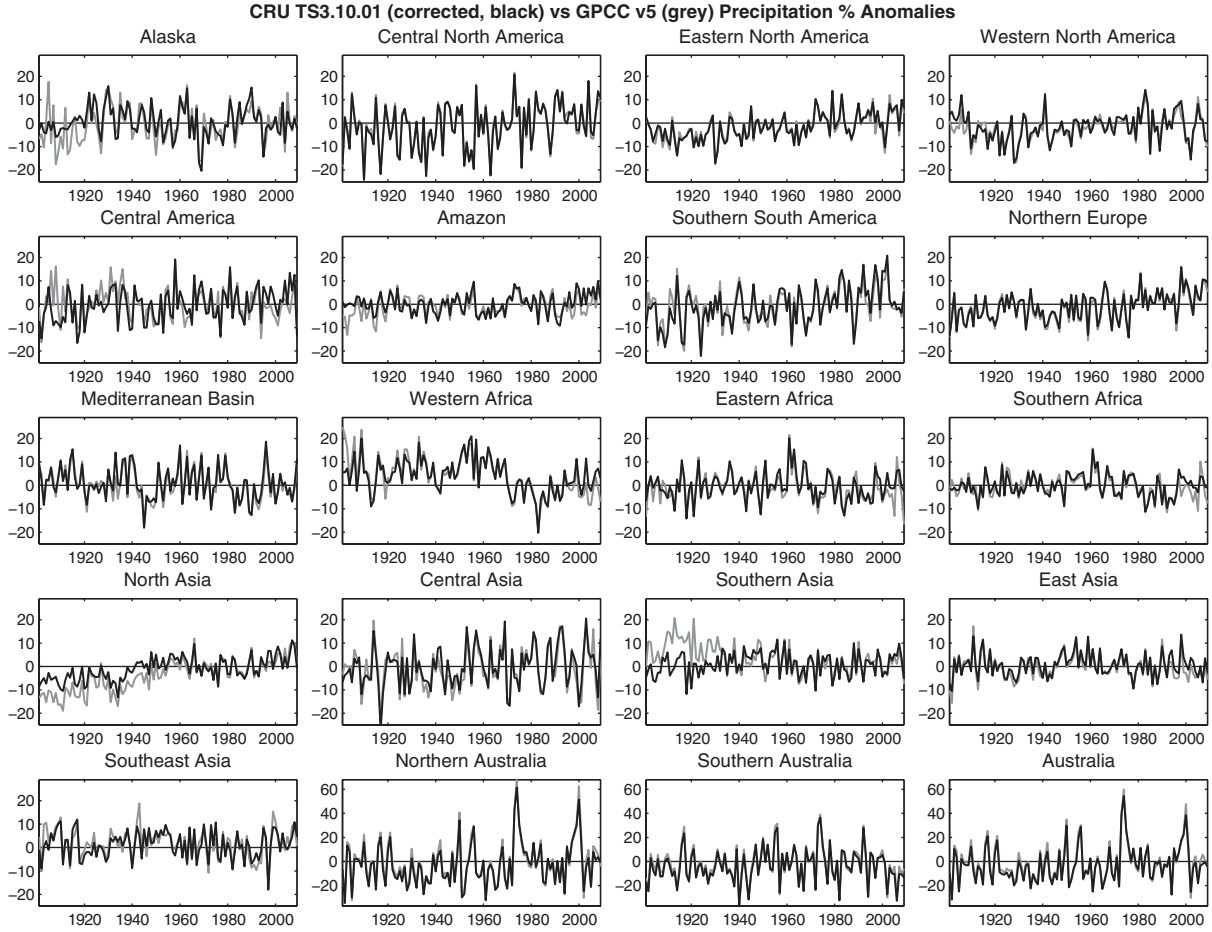

Figure 7. Regional comparisons between CRU TS3.10 (black lines) and GPCC v5 (grey lines) for total annual precipitation anomalies (mm), 1901 – 2009 from the base period of 1961–90, using the same scale for all regions except the Australian regions.

TS3.10 is also warmer than CRUTEM3 during the 1935–1950 period (warming was strongest in the high latitudes – e.g. Kuzmina *et al.*, 2008 – and interpolation can again explain differences between the two datasets). CRU TS3.10 annual temperature anomalies are also less negative than CRUTEM3 in some years earlier in the 20th century, possibly because interpolation includes zero anomalies in a few regions where there are no early observations within the CDD from the centre of a grid cell.

For the SH, the latter effect explains most of the differences between CRU TS3.10 and CRUTEM3 – i.e. infilling with zero anomalies becomes increasingly common in the data sparse early decades, raising the negative anomalies closer to zero. This raises the CRU TS3.10 temperature anomalies for the period before the 1940s, and the difference between the series gradually widens back to the start of the comparison in 1901. This leads to a smaller SH warming trend in CRU TS3.10 compared with CRUTEM3 (Table 1). It is not possible to completely exclude the effects of the zero anomalies (using, for instance, the station count files to mask out those regions prior to averaging), because the gridding process means that their influence spreads into the region within the CDD from an observed value, in cases where dummy stations with zero anomalies form one or two vertices of a triangle used for interpolation.

For comparison with CRUTEM4, CRU TS3.10 mean temperatures were spatially aggregated to a $5^\circ \times 5^\circ$ grid (matching that of CRUTEM4). For each cell with data values in both datasets, annual anomalies were constructed. Linear temporal trends were calculated for each cell of each dataset, and their gradients compared taking into account their 95% confidence limits (adjusted for autocorrelation). For the periods 1901–1950 and 1951–2009, only one cell in each test indicated that the temporal trends were inconsistent (i.e. the error estimates of the trends did not overlap). For the full, 1901–2009 period, two cells failed. Results from the CRUTEM4 comparisons can be found in supporting information.

4.3.2. Precipitation

Precipitation is again compared with the GPCC v5 half-degree gridded product (see Section 4.1), and the hemispheric and global results are shown in Figure 10. The overall (1901–2009) correlations are about 0.85 for the NH and SH, and 0.87 globally (Table 2). The two datasets are in closest agreement in the period of highest station density for CRU TS3.10 (Figures 3 and 4) and

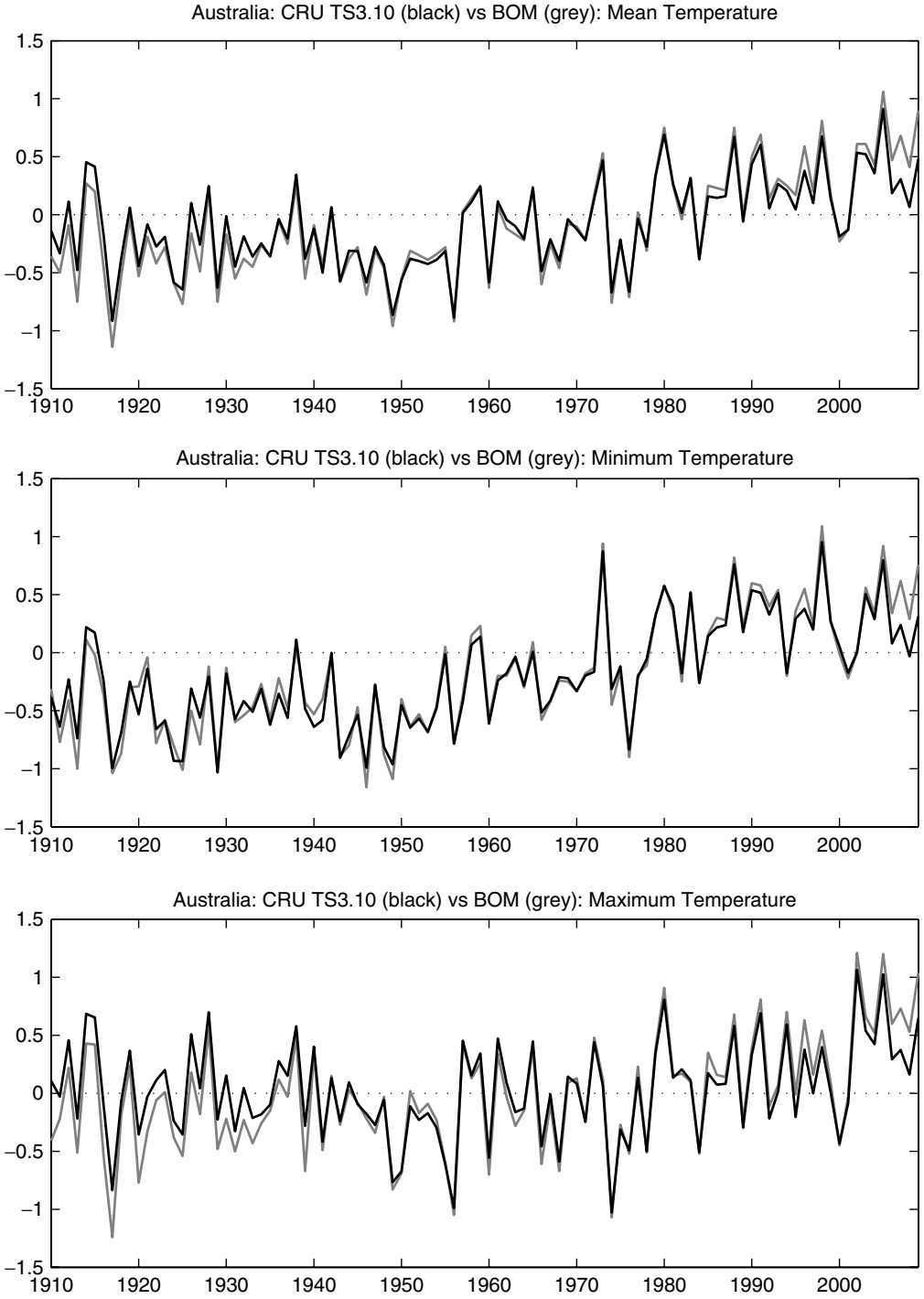

Figure 8. Comparisons between CRU TS3.10 (black) and BoM (grey) for mean, minimum and maximum annual temperature anomalies (°C) for Australia, 1910–2009. The base period is 1961–90.

the correlations increase to 0.88 or higher when the comparison is restricted to 1951–2009.

Nearly all CRU TS3.10 annual-mean average NH precipitation anomalies are higher (wetter) than the GPCC data prior to about 1957. This may arise for the reasons discussed in relation to the temperature comparison, that periods with sparser data coverage have an increased tendency towards zero anomalies in CRU TS3.10, which can make the anomalies less negative in dry regions and years. However, in the NH mean, CRU TS3.10 has *positive* (wet) anomalies in many of the pre-1957 years. Inspection of the sub-continental regions (Figure 7) identifies North Asia as the key NH region where the two datasets differ in their mean levels before 1957, with a smaller contribution from Alaska and an opposite contribution from Southern Asia before 1930. The North Asia precipitation trend is significantly stronger in the GPCC data (Table 2) and contributes greatly to the negative NH anomalies before 1950 in that dataset. Differences between precipitation trends in this

Table 3. CRU TS3.10 and BoM long-term trends for Mean, Maximum and Minimum Temperatures (°C/decade) for Australia. Trends significant at the 95% level are given in bold. Trends are calculated as for Table 1.

Australia: 1910–2009	Trends		Corr.
	CRU TS	BoM	
Mean temperature	**0.07**	**0.10**	0.87
Minimum temperature	**0.10**	**0.12**	0.98
Maximum temperature	0.03	**0.08**	0.94

region have been noted before. For example, Trenberth *et al.* (2007; compare their Figure 3.14 with our Figure 7) show a discrepancy between the GHCN dataset and CRU TS2.1 in North Asia. This region is particularly affected by undercatch of snow by raingauges, and long-term trends can be affected by changes in raingauge design or a shift in precipitation phase from snow to rain, and by application of adjustments to compensate for these potential inhomogeneities (Legates and Willmott, 1990; Groisman *et al.*, 1991).

As for temperature, we additionally compare CRU TS 3.10 precipitation trends with GPCCv5 trends for the same periods as in Section 4.3.1. (namely, 1901–50, 1951–2009 and 1901–2009). For all three periods for precipitation we find there are no cells indicating that the trend confidence intervals for each cell do not overlap each other. The results for these comparisons can also be found in the supporting information.

4.3.3. Diurnal Temperature Range (DTR)

A possible large-scale decline in DTR since the 1950s has received some attention in the climatological literature (Easterling *et al.*, 1997; Vose *et al.*, 2005). Trends in hemispheric and global-mean DTR are calculated from this analysis (CRU TS3.10) for the same periods 1951–2004 and 1979–2004 used by Vose *et al.* (2005). These are compared (Table 4) with the annual-mean DTR trends reported by Vose *et al.* (2005). In conducting the comparison, it was noticed that some of the seasonal and annual trends given by Vose *et al.* (2005) had the wrong sign. Revised trend values have been obtained (Russell Vose, pers. comm. via email, 15 November 2010) and agree very well with the present study.

5. Conclusions

We have produced a high-resolution global dataset of monthly climate observations, covering all land masses between 60°S and 80°N at a 0.5° x 0.5° resolution. Ten variables are included: precipitation, mean temperature, diurnal temperature range, minimum and maximum temperature, vapour pressure, cloud cover, rain days, frost days and potential evapotranspiration (PET). The period covered by the results shown here is from January 1901 to December 2009, though we have developed improved procedures to facilitate more frequent updates beyond 2009.

The dataset is derived from archives of climate station records that have been subject to extensive manual and semi-automated quality control measures. Records have been augmented with newly acquired data, and records/values of poor or suspect quality removed. Only station records with valid data covering at least three-quarters of the years between 1961 and 1990 are used, as this is the period from which station normals are calculated.

The station record archives are assembled from station networks that are spatially incomplete with respect to the full land surface. Interpolation within the Correlation Decay Distances (CDDs, MJ05) of stations allows nearly the entire land surface to be included for those 'primary' variables with widespread station networks (precipitation, temperature, temperatures). Variables with less observational coverage ('secondary' variables, such as vapour pressure) are augmented with synthetic data derived algorithmically from primary variables. Frost days and PET are entirely derived from other variables, as opposed to any direct measurements. Where land cells are beyond the reach of any station's CDD radius, the value reverts to the 1961–1990 climatology (from New *et al.*, 1999, which is unchanged from earlier versions of the dataset).

The dataset comprises a set of data files, and two companion sets of data coverage diagnostic files, which indicate the way in which each datum (a single value in one spatial cell at one timestep) in the data files was derived. The station influences files ('stn') enumerate the number of reporting stations within the appropriate CDD of the cell in question. The station counts files ('st0') give a count of the reporting stations located inside the boundaries of the cell. In both cases, 'reporting' means that an actual value is reported at that timestep and has not been excluded as a potential outlier.

Regional comparisons with other published datasets show that CRU TS3.10 temperatures agree tightly with the UDEL dataset. Close agreement for precipitation was also demonstrated between CRU TS3.10 and the GPCC dataset in many sub-continental regions, except for the first 50 years (1901–1950) when agreement is poorer in those regions with lower precipitation station density in CRU TS3.10 than in GPCC. In North Asia, there is a very clear difference in precipitation trend between the two datasets, mostly during the 1901–1950 period, which is sufficiently strong to affect the Northern Hemisphere and global comparisons as well. For temperature, the Northern Hemisphere mean agrees well with the CRUTEM3 (Brohan *et al.*, 2006) dataset (much of the station data is common to both datasets, though the methods of gridding the data are different) but the less well sampled Southern Hemisphere shows differences before 1950 that are associated with the infilling of zero anomaly values in CRU TS3.10 in regions with few observed station data.

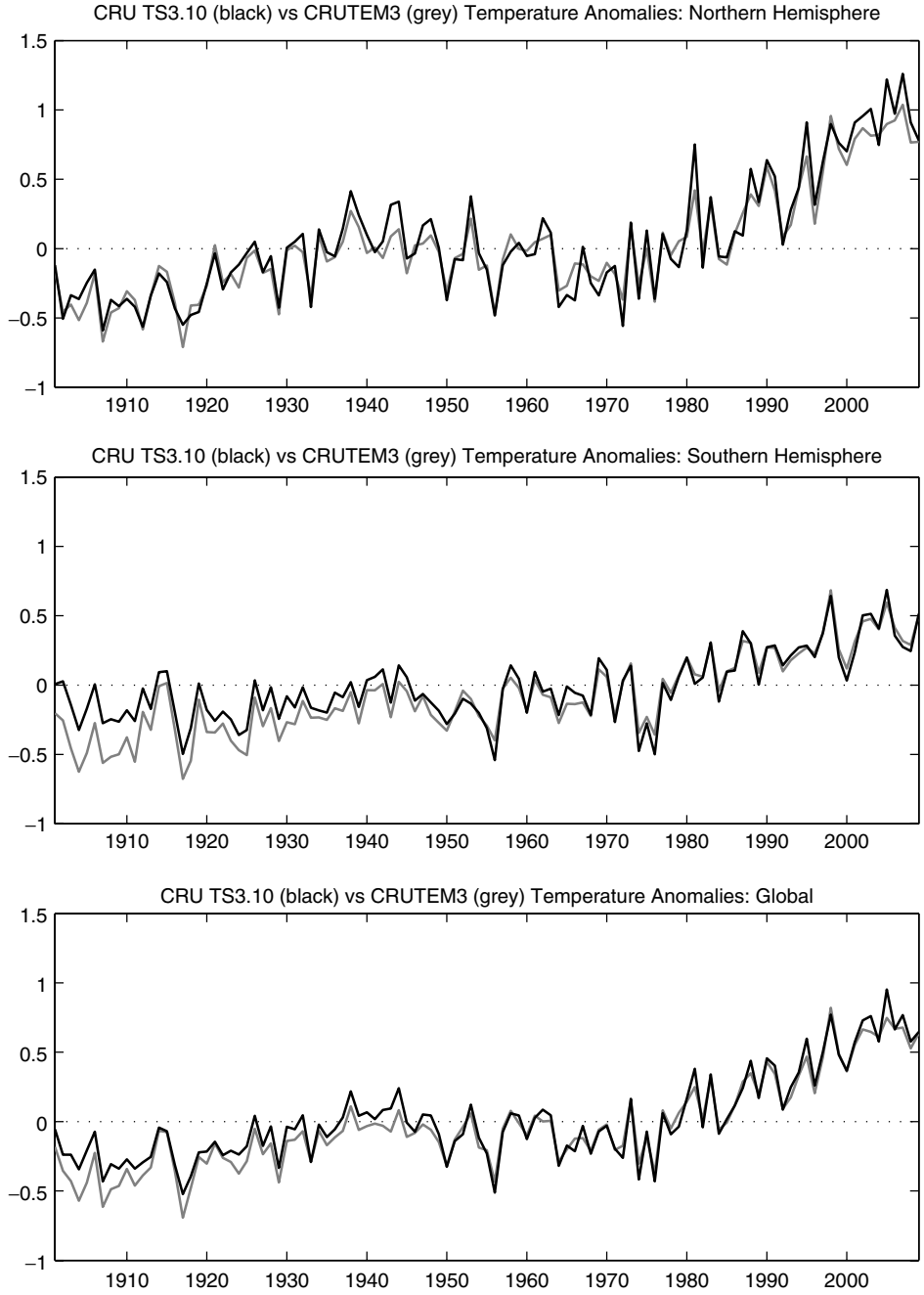

Figure 9. Hemispheric and global comparisons between CRU TS3.10 (black lines) and CRUTEM3 (grey lines) for annual temperature anomalies (°C), 1901–2009. The base period is 1961–90.

The current CRU TS3.10 dataset is an update to the previous versions of the CRU TS dataset (1.0, 2.0, 2.10 and 3.00). These versions all differ in the time periods covered and in the contents of the station observations databases that are used. There are also differences in the details of the methods used to process and grid the datasets, and in the implementation of those processes as computer software. From CRU TS3.00 onwards, the implementation of the processes has been simplified in order to allow automation, though this was not put into operation until CRU TS3.10. The process by which the dataset is produced has been recorded (e.g. Figures 1,2 and 5) and composed as a software suite, which may be executed to produce updated datasets with minimal operator intervention. The run-level program allows both the updating of the databases of observations (using updates from MCDW, CLIMAT and BOM), and the subsequent production of updated gridded datasets. Differences from CRU TS3.00 to CRU TS3.10 reflect incremental improvements in the underlying station databases. The gridded data, along with the monthly station observations for TMP, TMN, TMX and DTR, are freely available at the British Atmospheric Data Centre website (http://badc.nerc.ac.uk/view/badc.nerc.ac.uk_ATOM_dataent_1256223773328276).

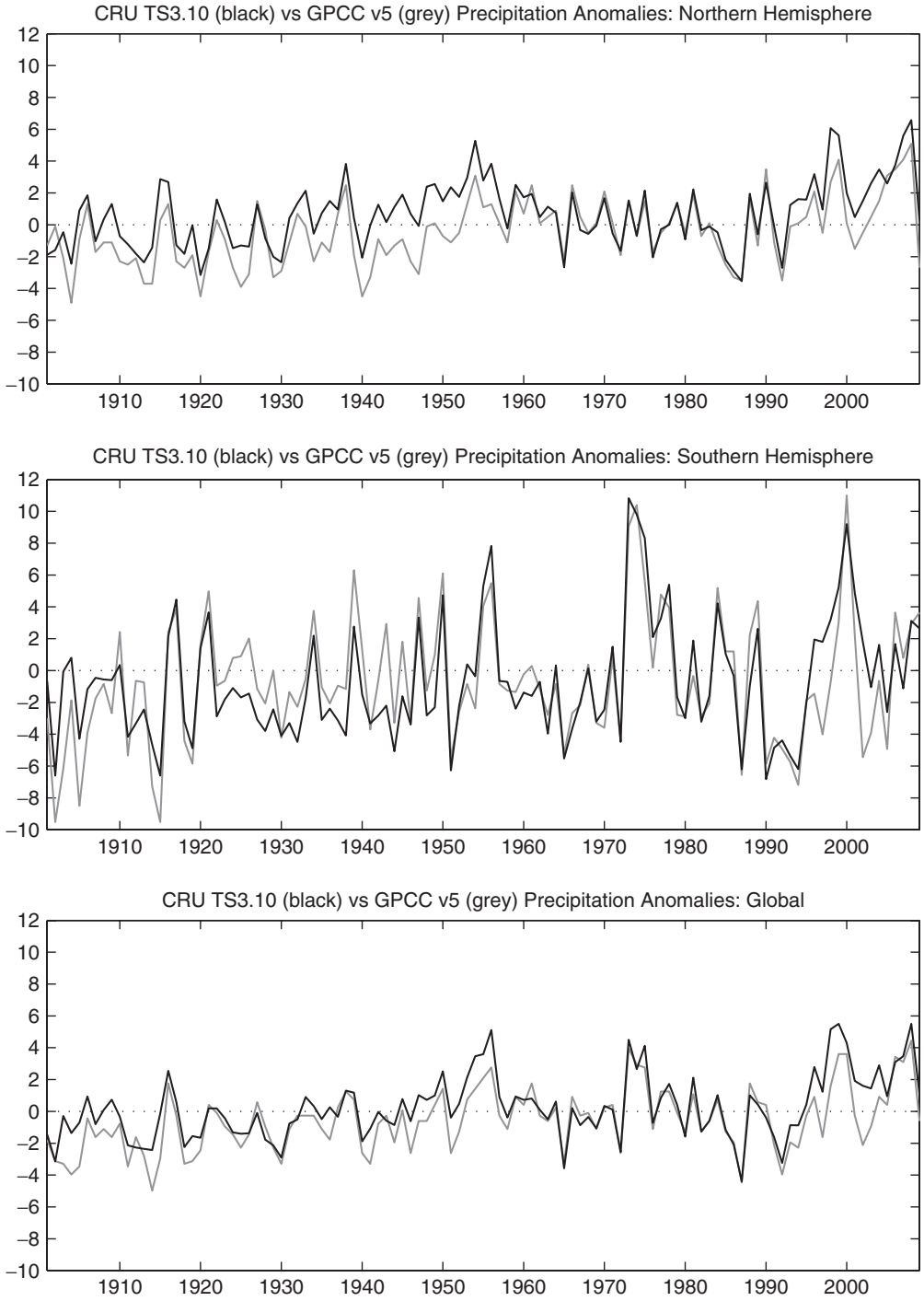

Figure 10. Hemispheric and global comparisons between CRU TS3.10 (black lines) and GPCC v5 (grey lines) for annual total precipitation percentage anomalies, 1901–2009. The base period is 1961–90.

Table 4. CRU TS3.10 long-term trends in hemispheric and global Diurnal Temperature Range (°C/decade) compared with figures (some corrected, see Section 4.3.3) from Vose *et al.* (2005). Trends significant at the 95% level are given in bold. Trends are calculated as for Table 1.

Region	1950–2004		1979–2004	
	Vose *et al.* (2005)	CRU TS	Vose *et al.* (2005)	CRU TS
Global	**−0.07**	**−0.07**	−0.00	**−0.03**
Northern Hemisphere	**−0.08**	**−0.08**	−0.03	**−0.03**
Southern Hemisphere	**−0.03**	**−0.03**	0.05	−0.02

Acknowledgements

The authors wish to thank David Jones, BoM; Jim Renwick, New Zealand National Institute of Water and Atmospheric Research (NIWA); Russ Vose, NCDC; Lucie Vincent, Atmospheric Environment Service (AES), Canada, for the provision of additional station data (sometimes homogenized). David Jones has also arranged to send BoM data routinely each month. This project has been supported by the British Atmospheric Data Centre, CCLRC (now called STFC) Contract No. 4146417, the NERC QUEST project (QUEST GSI, NE/E001890/1), the European Union, Seventh Framework Programme (FP7/2007-2013) under grant agreement no. 242093 (EURO4M).and the development of the station climate datasets over the years has been supported by the Office of Science (BER), US Dept. of Energy, Grant No. DE-SC0005689.

Appendix 1: PET calculation

Potential evapotranspiration (PET) is an important variable in hydrological modelling. Here a variant of the Penman–Monteith method is used (Eq. A1): the FAO (Food and Agricultural Organization) grass reference evapotranspiration equation (Ekström *et al.*, 2007, Eq. 1 which is based on Allen *et al.*, 1994, Eq. 2.18). The FAO Penman–Monteith method defines PET as the potential evapotranspiration from a clipped grass-surface having 0.12 m height and bulk surface resistance equal to $70\,\mathrm{s\,m^{-1}}$, an assumed surface albedo of 0.23 (Allen *et al.*, 1994), and no moisture stress. Measurements of meteorological variables are assumed to be at a height of 2 m, apart from the wind (10 m). To overcome the height difference for the wind variable, a conversion coefficient (computed as 0.7471) was used to reduce the 10 m wind to the 2 m wind height required for PET calculation, based on the logarithmic wind profile (Allen *et al.*, 1994):

$$\mathrm{PET} = \frac{0.408\Delta\,(R_n - G) + \gamma\,\frac{900}{T+273.16}U_2\,(e_a - e_d)}{\Delta + \gamma\,(1 + 0.34U_2)} \tag{A1}$$

where

$$U_2 = U_{10}\frac{\ln(128)}{\ln(661.3)}$$

and PET: reference crop evapotranspiration [$\mathrm{mm\,d^{-1}}$]; R_n: net radiation at crop surface [$\mathrm{MJ\,m^{-2}\,d^{-1}}$]; G: soil heat flux [$\mathrm{MJ\,m^{-2}\,d^{-1}}$]; T: average temperature at 2 m height [°C]; U_2: windspeed measured (or estimated from U_{10}) at 2 m height [$\mathrm{m\,s^{-1}}$]; U_{10}: windspeed measured at 10 m height [$\mathrm{m\,s^{-1}}$]; $(e_a - e_d)$: vapour pressure deficit for measurement at 2 m height [kPa]; Δ: slope of the vapour pressure curve [$\mathrm{kPa\ ^\circ C^{-1}}$]; γ: psychrometric constant [$\mathrm{kPa\ ^\circ C^{-1}}$]; 900: coefficient for the reference crop [$\mathrm{kJ^{-1}\,kg\,K\ d^{-1}}$], Allen *et al.* (1994); 0.34: wind coefficient for the reference crop [$\mathrm{s\,m^{-1}}$] (Allen *et al.*, 1994).

In the calculation of PET, we need absolute values of all the variables. These are produced by adding or multiplying back by the 1961–1990 baseline values. For wind, we do not have anomaly time series, so use time-invariant values (i.e. the same 1961–1990 monthly values for each month in each year).

Appendix 2: Formulae for converting between absolute values and anomalies

Regular anomalies:

$$x = x_a + \overline{x} \tag{A2}$$

Percentage anomalies:

$$x = \frac{x_a\ \overline{x}}{100} + \overline{x} \tag{A3}$$

where: x is the absolute value; $\overline{x}$ is the normal, or mean value over the reference period; x_a is the anomaly.

Appendix 3: Formulae used to convert between variables

TMN, TMX and DTR

Station DTR is calculated from station TMN and TMX according to:

$$\mathrm{DTR} = \mathrm{TMX} - \mathrm{TMN} \tag{A4}$$

Gridded TMN and TMX are derived from gridded TMP and DTR according to:

$$\mathrm{TMN} = \mathrm{TMP} - \frac{\mathrm{DTR}}{2} \tag{A5}$$

$$\mathrm{TMX} = \mathrm{TMP} + \frac{\mathrm{DTR}}{2} \tag{A6}$$

VAP

Synthetic VAP is estimated from DTR and TMP anomalies, using TMN (calculated as (TMP − (DTR/2)) as a proxy for TDEW (the dewpoint temperature, New *et al.*, 1999; MJ05). TDEW normal is calculated from VAP normal, then TMN normal is adjusted so that the average is equal to the TDEW normal. Synthetic VAP (hPa) is constrained to lie between 0.1 and saturated VAP at mean temperature.

$$\mathrm{VAP} = 6.108 * \mathrm{e}^{\frac{17.27*\mathrm{TMN}}{237.3+\mathrm{TMN}}} \tag{A7}$$

WET

Synthetic WET is calculated from PRE, and PRE and WET normal climatologies (for the period 1961–1990 and termed $\overline{\mathrm{PRE}}$_NORM and $\overline{\mathrm{WET}}$_NORM respectively). The formula below has been used previously (New *et al.*, 2000; MJ05). This synthetic WET is combined with observed WET at the gridding stage.

$$\mathrm{WET} = \left(\frac{\mathrm{PRE} * \overline{\mathrm{WET}}^{\frac{1}{0.45}}}{\overline{\mathrm{PRE}}}\right)^{0.45} \tag{A8}$$

CLD

Cloud percentage cover is derived from observations of sun hours as follows:

Firstly, sun hours is converted to sun fraction, using monthly declination constants and 'maximum possible sunshine hours' estimates from Table 3 in Doorenbos and Pruitt (1984). Secondly, sun percent is converted to cloud cover oktas*10. The relationship is negative and piecewise-linear, with conditionals determining the relationship for different values of sun hours (expressed as a fraction, 'srat'):

if srat>= 0.95, cloud cover=0.0
if 0.95<srat<=0.35, cloud cover=(0.95-srat)*100
if 0.35<srat<=0.15, cloud cover=((0.35-srat)*50 +60)
if 0.15<srat<0.00, cloud cover=((0.15-srat)*100 +70)
cloud cover is then capped at 80 (oktas*10)

Finally, cloud cover percent is derived by multiplying the okta*10 values by 1.25.

Synthetic CLD anomalies at each station are estimated from station DTR anomalies, using pre-calculated monthly coefficients (factors and offsets) for each half-degree latitude band.

$$\mathrm{CLD} = \left(\mathrm{DTR} * \mathrm{factor}_j\right) + \mathrm{offset}_j \qquad \text{(A9)}$$

where j = grid box latitude, and the factors and offsets were calculated from CRU TS2.10 gridded CLD and DTR values for each latitude band.

FRS

Synthetic FRS is calculated from TMN (as derived from TMP and DTR). This formula is given in New *et al.* (2000) and MJ05.

$$\mathrm{FRS} = 50 * \cos\left(\tfrac{180}{24} * ((\mathrm{TMN} + 14) - |12 - |x + 2|| * 0.32) * \tfrac{\pi}{180}\right) + 50 \quad \text{where } [-14 < \mathrm{TMN} < 10] \qquad \text{(A10)}$$

When TMN ≤ -14, then FRS is the number of days in the month.

Note that, for CRU TS3.10, this process was complicated by being applied to anomalies. This can result in unrealistic FRS absolute values when compared to TMN absolute values. Therefore, the next version of the dataset will apply the above process to gridded absolute values of TMN.

References

Allen RG, Smith M, Pereira LS, Perrier A. 1994. An update for the calculation of reference evapotranspiration. *ICID Bulletin* **43**: 35–92.

Becker A., Finger P, Meyer-Christoffer A, Rudolf B, Schamm K, Schneider U, Ziese M. 2013. A description of the global land-surface precipitation data products of the Global Precipitation Climatology Centre with sample applications including centennial (trend) analysis from 1901-present. *Earth System Science Data* **5**: 71–99. 10.5194/essd-5-71-2013

Brohan P, Kennedy J, Harris I, Tett SFB, Jones PD. 2006. Uncertainty estimates in regional and global observed temperature changes: a new dataset from 1850. *Journal of Geophysical Research* **111**: D12106. DOI: 10.1029/2005JD006548

Doorenbos J, Pruitt WO. 1984. Guidelines for predicting crop water requirements. Food and Agriculture Organization of the United Nations (FAO) Irrigation and Drainage Paper 24.

Easterling DR, Horton B, Jones PD, Peterson TC, Karl TR, Parker DE, Salinger MJ, Razuvayev V, Plummer N, Jamason P, Folland CK. 1997. A new look at maximum and minimum temperature trends for the globe. *Science* **277**: 364–367.

Ekström M, Jones PD, Fowler H, Lenderink G, Buishand TA, Conway D. 2007. Regional climate model data used within the SWURVE project 1: projected changes in seasonal patterns and estimation of PET. *Hydrology and Earth Systems Science* **11**: 1069–1083.

Giorgi F, Francesco R. 2000. Evaluating uncertainties in the prediction of regional climate change. *Geophysical Research Letters* **27**: 1295–1298.

Groisman PY, Koknaeva VV, Belokrylova TA, Karl TR. 1991. Overcoming biases of precipitation: a history of the USSR experience. *Bulletin of the American Meteorological Society* **72**: 1725–1733.

Hofstra N, Haylock MR, New M, Jones PD, Frei C. 2008. Comparison of six methods for the interpolation of daily European climate data. *Journal of Geophysical Research* **113**: D21110. DOI: 10.1029/2008JD010100

Jones PD, Osborn TJ, Briffa KR. 1997. Estimating sampling errors in large-scale temperature averages. *Journal of Climate* **10**: 2548–2568.

Jones PD, Osborn TJ, Briffa KR, Folland CK, Horton B, Alexander LV, Parker DE, Rayner NA. 2001. Adjusting for sample density in grid-box land and ocean surface temperature time series. *Journal of Geophysical Research* **106**: 3371–3380.

Jones PD, Lister DH, Osborn TJ, Harpham C, Salmon M, Morice CP. 2012. Hemispheric and large-scale land surface air temperature variations: an extensive revision and an update to 2010. *Journal of Geophysical Research* **117**: D05127. DOI: 10.1029/2011JD017139

Kuzmina SI, Johannessen OM, Bengtsson L, Aniskina OG, And Bobylev LP. 2008. High northern latitude surface air temperature: comparison of existing data and creation of a new gridded data set 1900–2000. *Tellus A* **60**: 289–304. DOI: 10.1111/j.1600-0870.2008.00303.x

Legates DR, Willmott CJ. 1990. Mean seasonal and spatial variability in gauge-corrected, global precipitation. *International Journal of Climatology* **10**: 111–127.

Mitchell TD, Jones PD. 2005. An improved method of constructing a database of monthly climate observations and associated high-resolution grids. *International Journal of Climatology* **25**: 693–712.

New M, Hulme M, Jones PD. 1999. Representing twentieth-century space-time climate variability. Part I: development of a 1961-90 mean monthly terrestrial climatology. *Journal of Climate* **12**: 829–856.

New M, Hulme M, Jones PD. 2000. Representing twentieth century space-time climate variability. II: development of 1901–1996 monthly grids of terrestrial surface climate. *Journal of Climate* **13**: 2217–2238.

Nicholls N, Tapp R, Burrows K, Richards D. 1996. Historical thermometer exposures in Australia. *International Journal of Climatology* **16**: 705–710.

Peterson TC, Vose RS. 1997. An overview of the global historical climatology network temperature database. *Bulletin of the American Meteorological Society* **78**(12): 2837–2849.

Peterson TC, Karl TR, Jamason PF, Knight R, Easterling DR. 1998a. The first difference method: maximizing station density for the calculation of long-term global temperature change. *Journal of Geophysical Research* **103**: 25967–25974.

Peterson TC, Vose RS, Schmoyer R, Razuvaev V. 1998b. Global Historical Climatology Network (GHCN) quality control of monthly temperature data. *International Journal of Climatology* **18**: 1169–1179.

Schneider U, Becker A, Finger P, Meyer-Christoffer A, Ziese M, Rudolf B. 2013. GPCC's new land surface precipitation climatology based on quality-controlled in situ data and its role in quantifying the global water cycle. *Theoretical and Applied Climatology* http://dx.doi.org/10.1007/s00704-013-0860-x.

Trenberth KE, Jones PD, Ambenje P, Bojariu R, Easterling D, Klein Tank A, Parker D, Rahimzadeh F, Renwick JA, Rusticucci M, Soden B, Zhai P. 2007. Observations: surface and atmospheric

climate change. In *Climate Change 2007: The Physical Science Basis*. Contribution of Working Group 1 to the Fourth Assessment Report of the Intergovernmental Panel on Climate Change, Solomon S, Qin D, Manning M, Chen Z, Marquis M, Averyt KB, Tignor M, Miller HL (eds). Cambridge University Press: Cambridge and New York, NY; 235–336.

Vincent LA. 1998. A technique for the identification of inhomogeneities in Canadian temperature series. *Journal of Climate* **11**: 1094–1104.

Vincent LA, Gullet DW. 1999. Canadian historical and homogeneous temperature datasets for climate change analyses. *International Journal of Climatology* **19**: 1375–1388.

Vose RS, Easterling DR, Gleason B. 2005. Maximum and minimum temperature trends for the globe: an update through 2004. *Geophysical Research Letters* **32**: L23822. DOI: 10.1029/2004GL024379

Willmott CJ, Robeson SM. 1995. Climatologically Aided Interpolation (CAI) of terrestrial air temperature. *International Journal of Climatology* **15**: 221–229.

